One-Dimensional Soft-Demapping Algorithms for Rotated QAM and Software Implementation on DSP

Kyeongyeon Kim, *Member, IEEE*, Navneet Basutkar, Kitaek Bae, *Member, IEEE*, Peng Xue, *Member, IEEE*, and Ho Yang, *Member, IEEE*

***Abstract*—To improve detection performance of quadrature amplitude modulation (QAM), signal space diversity (SSD) has been exploited and adopted for the second generation of digital video broadcasting (DVB-T2) system. Maximum-likelihood detection (MLD) to get full SSD is avoided because of enormous computational complexity. Its max-log approximated detection (full search algorithm) and subregion based soft-demappers are also too complex to be implemented due to their two-dimensional (2D) Euclidean distance calculation. In particular, the complexity becomes the main burden for the software implementation, which is attractive for multistandard broadcasting receivers. To tackle the main bottleneck, we propose one-dimensional (1D) soft-demappers. By reformulating a rotated QAM signal as two layered pulse amplitude modulation (PAM) signals, the full search algorithm is simplified to an MMSE decorrelation followed by 1D soft-demapping, where Gaussian approximation is used for the interferences. Additional interference cancellation is considered to further suppress its residual interference. For 256-QAM with 4/5 code rate in memoryless Rayleigh channels with/without erasures, the performance gap to the full search is within 0.15 dB at 10^{-3} bit error rate (BER), while the complexity is less than 8%. Due to the significant complexity reduction of the proposed algorithms, the software implementation of a DVB-T2 receiver on DSP is feasible with 73% less computations than the one with the full-search-based soft-demapper.**

***Index Terms*—Coarse-grained reconfigurable array (CGRA) architecture, digital signal processor (DSP), interference cancellation (IC), log likelihood ratio (LLR), minimum mean square error (MMSE), rotated QAM, signal space diversity (SSD), soft-demapping, software defined radio (SDR).**

I. Introduction

SIGNAL SPACE DIVERSITY (SSD) (or modulation diversity) was introduced in [1], [2], to improve spectral efficiency and bit error rate (BER) performance over fading channels. Firstly, a quadrature amplitude modulation (QAM) in a signal space is rotated with a particular angle, and then one of the in-phase (I) or quadrature (Q) components of the signal is interleaved with respect to the other. The interleaving can be simply implemented with a cyclic Q delay and a symbol interleaver. The rotated QAM with cyclic Q delay combined with several interleavers was adopted for the second generation of terrestrial digital video broadcasting (DVB-T2) system [3], and provides improvement in BER performance especially in the presence of erasure events as shown in [4].

However, the complexity of its soft-demapping (i.e., log likelihood ratio (LLR) calculation) for the rotated QAM with cyclic Q delay is extremely high. Unlike soft-demappers of a non-rotated QAM, the maximum likelihood (ML) detector can not be simplified into two independent pulse amplitude modulation (PAM) detectors any more, because the rotated QAM with cyclic Q delay makes correlation between I and Q components of the received QAM signal. Even though max-log approximation can be used for the soft-demapping [5], [6], it still requires Euclidean distance calculation from a received signal point to all the constellation points in two dimensional (2D) signal space. Therefore, the max-log approximated soft-demapper for the rotated QAM requires 2^m 2D Euclidean distance calculations[1] in the 2^m-QAM case, while its corresponding non-rotated QAM soft-demapping requires only $2^{(m/2)+1}$ one-dimensional (1D) Euclidean distance calculations.

To reduce the complexity of the rotated QAM soft-demapping, sub-region based algorithms according to the sign information of both I and Q components of a received QAM signal are proposed [7], [8]. In [7], a rotated-L-shape sub-region is considered based on empirical histogram analysis. The complexity of the soft-demapping is reduced at most 50% of the full search algorithm according to various scenarios (e.g., subset 1, $\cdots$, subset 5). When a square-shape sub-region is considered [8], the soft-demapping algorithm reduces its complexity to 40% of the full search algorithm for a 64-QAM case. With approximation in Euclidean distance calculation, the complexity is reduced up to 20%. The selected (full or reduced) set can be reused for LLR calculations of all the bits. In [9], per dimension demapper (PD-DEM) selects only two sectors (i.e., $2^{m/2}$ constellation points) closest to the received signal for LLR calculation of each bit. Compared to other sub-region based algorithms, however, the complexity reduction in PD-DEM is not that much due to the limitation in the reusability of the calculated Euclidean distances. As other low complexity algorithms for the rotated QAM soft-demapping, hybrid algorithms (i.e., the combination of soft and hard outputs) are proposed [10]. Hard decision is made for reliable bits, where there are four different hybrid algorithms based on the criteria for the reliability. However, the computational benefit of these hybrid algorithms is small in low signal-to-noise ratio (SNR) region and the hybrid algorithms require additional soft output calculation of the

Manuscript received September 11, 2012; revised January 11, 2013 and April 14, 2013; accepted April 17, 2013. Date of publication May 13, 2013; date of current version July 10, 2013. The associate editor coordinating the review of this manuscript and approving it for publication was Prof. Tong Zhang.

The authors are with Samsung Advanced Institute of Technology (SAIT), Samsung Electronics, Yongin-si Gyeonggi-do, South Korea (e-mail: kyeongyeon.kim@samsung.com; navneet.basutkar@samsung.com; kitaek.bae@samsung.com; peng.xue@samsung.com; and hoyang@samsung.com).

Digital Object Identifier 10.1109/TSP.2013.2262681

[1]In this paper, we call this max-log approximated soft-demapper as a full search algorithm.

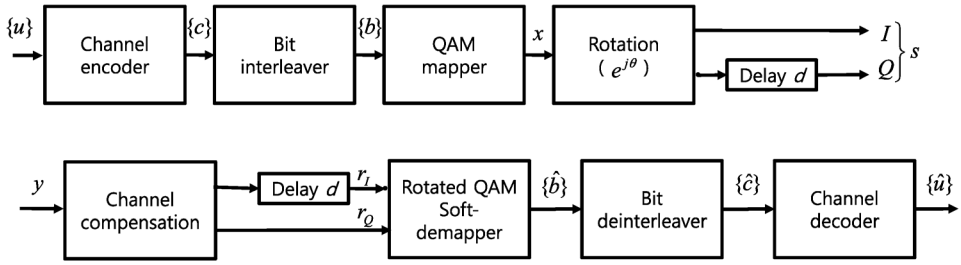

Fig. 1. System block diagram for bit-interleaved coded modulation (BICM) with SSD using Rotated QAM.

hard decision bits to get proper low density parity check (LDPC) decoding input. Even though the low complexity algorithms reduce the complexity compared to the full search algorithm, those algorithms still require 2D Euclidean distance calculation and the complexity increases with the higher modulation order. Such complexity increase can be a bottleneck especially for full software implementation desired for flexible and programmable radio platforms to support multi-standards. Using the in-house DSP based on a coarse-grained reconfigurable array (CGRA) architecture [11], [12], the required cycle counts of core kernels[2] of the DTG106 mode[3] [13] in the DVB-T2 system showed 516 Mega cycles per second (Mcps)[4] in [14]. Even with the soft-demapper for a non-rotated 256-QAM, the soft-demapper accounts for about 25% of total core kernel cycle counts. Note that the complexity of the full search based soft-demapper for a rotated 256-QAM is over 60 times higher than the non-rotated QAM soft-demapper. The software implementation is impractical due to the high complexity even with the existing sub-region based soft-demappers.

In this paper, we propose new low complexity soft-demapping algorithms to reduce its complexity as low as the soft-demapper for the non-rotated QAM. Firstly, we reformulate a received rotated QAM signal with cyclic Q delay as two PAM signals. Due to Gaussian approximation on the post detected PAM signals, the ML detector for the rotated QAM with cyclic Q delay is simplified to a 2×2 unbiased MMSE (U-MMSE) decorrelation followed by per-component soft-demapping (i.e., 1D soft-demapping). After the MMSE decorrelation, further interference cancellation (IC) can be taken into account to reduce the residual interference from the other channel. By the characteristic of the rotation matrix, the proposed algorithm does not require matrix inversion. In addition, the order of IC can be decided in advance, which makes implementation easily parallelized by moving conditional execution outside a main loop forming a separated loop and calculating LLR values in two individual loops. Moreover, the 1D soft-demapping can be simplified by either table based LLR calculation [15], [16] or LLR calculation using predefined closest points [17] as in a non-rotated QAM. To show the feasibility of software implementation for a DVB-T2 receiver, the proposed algorithms are mapped on the CGRA processor and compared to the cycle counts of the existing algorithms.

The remainder of this paper is organized as follows. Section II overviews the basic principles of the SSD and introduces previous soft-demapping algorithms for the rotated QAM. Our new soft-demapping algorithms are proposed in Section III. The proposed algorithms are optimized on the CGRA processor. Key features of the CGRA processor and the optimization points are summarized in Section IV. In Section V, the floating and fixed point BER performance of the proposed algorithms is evaluated and the complexity of the proposed algorithms is compared with the full search algorithm and its low complexity algorithms with sub-regions. Finally, Section VI gives concluding remarks.

II. Background of Soft-demapping Algorithms

A. Channel and Signal Models

For the transmited signal $s[n]$, the nth received signal $y[n]$ is given as

$$y[n] = h[n]s[n] + w[n], \tag{1}$$

where $h[n]$ is a memoryless Rayleigh fading channel coefficient, and $w[n]$ is an additive white Gaussian noise (AWGN) with variance σ_n^2. By introducing simple erasure channel events, the classical memoryless Rayleigh channel can be modified as follows.

$$y[n] = h[n]e[n]s[n] + w[n], \tag{2}$$

where $e[n]$ models random erasure events by taking 0 with a probability P_e, or 1 with a probability $1 - P_e$ under the assumption of infinite channel interleaving [4], [8]. The assumption is more appropriate, if the frame length is long enough and the bit and symbol interleavers are used at a transmitter side as in the DVB-T2 system.

B. Transceiver Structure of BICM with SSD

As shown in Fig. 1, $x[n] = x_I[n] + jx_Q[n]$ after QAM mapping, is rotated with a modulation specific angle θ. To get the SSD, the Q component is delayed, and then the new complex signal $s[n] \triangleq (x_I[n]\cos\theta - x_Q[n]\sin\theta) + j(x_Q[n - d]\cos\theta + x_Q[n - d]\sin\theta)$ is transmitted. At the receiver side, the I component of the phase compensated signal is delayed to

[2]These include most of functions (i.e., synchronization, 32 K FFT, channel estimation, equalization, de-interleaving and soft-demapping) in the baseband modem of a DVB-T2 system.

[3]This is one of the most likely candidates to be adopted for DVB-T2 services by Ofcom, which is the office of communications in UK. In this mode, 32 K FFT, 256-QAM, 3/5 code rate, 1/128 guard interval and PP7 (as pilot pattern) are used.

[4]This total cycle counts include direct memory access (DMA) cycles and additional 20% control overhead. Note that the mapped total cycle counts of core kernels are 334 Mcps with a soft-demapper for a non-rotated 256-QAM.

align I and Q components. Finally, the received signal, $r[n] = r_I[n-d] + jr_Q[n]$, can be restated as follows.

$$\begin{bmatrix} r_I[n-d] \\ r_Q[n] \end{bmatrix} = \mathbf{PQ} \begin{bmatrix} x_I[n-d] \\ x_Q[n-d] \end{bmatrix} + \begin{bmatrix} w_I[n-d] \\ w_Q[n] \end{bmatrix}, \quad (3)$$

where $\mathbf{P} \triangleq \begin{bmatrix} \rho_I & 0 \\ 0 & \rho_Q \end{bmatrix}$ and $\mathbf{Q} \triangleq \begin{bmatrix} \cos\theta & -\sin\theta \\ \sin\theta & \cos\theta \end{bmatrix}$, where $\mathbf{P}$ denotes a diagonal channel gain matrix and $\rho_I \triangleq \|h[n-d]e[n-d]\|$, in the case of $\rho_Q \triangleq \|h[n]e[n]\|$. The matrix $\mathbf{Q}$ means a rotation matrix defined by modulation specific angles.

For simplicity, we will omit the time indices from now on. By transmitting the rotated QAM signal with delayed Q component, both r_I and r_Q are formed as functions of both x_I and x_Q (i.e., correlated with each other) and undergo different channels, ρ_I and ρ_Q, respectively. We assume that the channel coefficients ρ_I and ρ_Q are independent to each other.[5] By using the independence of the channel coefficients and the signal correlation, SSD can be exploited [1], [2]. The optimal diversity gain can be achieved when the ML detector is used [2]. However, the complexity is extremely high especially with higher modulation orders such as 64-QAM or 256-QAM.

C. Previous Soft-Demapping Algorithms for Rotated QAM

To relieve high complexity of the ML detector, the max-log approximation is used [5], [6] as follows.

$$\Lambda(b_k) = \log \frac{\Pr[b_k = 0|r]}{\Pr[b_k = 1|r]} \quad (4)$$

$$= \log \frac{\sum_{a \in \mathcal{A}_k^0} \Pr[r|x=a]}{\sum_{a \in \mathcal{A}_k^1} \Pr[r|x=a]} \quad (5)$$

$$\approx \max_{a \in \mathcal{A}_k^0} \log \Pr[r|x=a] - \max_{a \in \mathcal{A}_k^1} \log \Pr[r|x=a] \quad (6)$$

$$= \lambda(r) \left(\min_{a \in \mathcal{A}_k^1} D(a) - \min_{a \in \mathcal{A}_k^0} D(a) \right), \quad (7)$$

where $D(a) \triangleq (r_I - \rho_I \cdot s_I(a))^2 + (r_Q - \rho_Q \cdot s_Q(a))^2$,
for $s_I(a) \triangleq a_I \cos\theta - a_Q \sin\theta$
and $s_Q(a) \triangleq a_I \sin\theta + a_Q \cos\theta$.

$\Pr[A|B]$ denotes the conditional probability of A given B and $a \triangleq a_I + ja_Q$ means a non-ratated QAM signal. In addition, $\lambda(r)$ is a scaling factor as a function of SNR. The equality (5) comes from Bayes' rule and equiprobable bit distribution (i.e., $\Pr[b_k = 0] = \Pr[b_k = 1]$). Finally, the max-log approximated LLR calculation as in (7) is simplified to distance metric for a Gaussian probability density function (pdf). However the algorithm still requires full search over the distance between a received signal and all possible constellation points in the sets $\mathcal{A}_k^1$ and $\mathcal{A}_k^0$, where $\mathcal{A}_k^1$ and $\mathcal{A}_k^0$ denote constellation sets when the kth bit information equals to 1 and 0, respectively.

To avoid full search, [7] and [8] propose sub-region based algorithms. They divide four sub-regions in the 2D signal space based on the sign of I and Q components in the received signal. The reference [7] proposes a rotated-L-shape sub-region based algorithm by analysing the histogram of the minimum Euclidean distances. For all the received points in a particular quadrant, the constellation symbols that are more likely to be at the minimum distance are determined based on the histogram. For example, all the received points in the first quadrant are more likely to be at the minimum distance with the constellation symbols in the first, second and fourth quadrants rather than third quadrant (i.e., rotated "L" shape). Therefore, the complexity of the rotated-L-shape sub-region based algorithm is about 50% $\sim$ 75% of the number of required operations compared with the full search algorithm, according to the kind of subsets at the cost of performance degradation. In [8], the authors consider four square-shape sub-regions. Since they allow the overlapping regions to take into account the rotated constellation, the algorithm has about 40% and 31% complexity of the full search algorithm in 64-QAM and 256-QAM cases, respectively.

Whereas, each metric in (7) can be calculated over $2^{m/2}$-PAM signal space (i.e., 1D signal space) in a general 2^m-QAM signalling (i.e., non-rotated QAM), because there is no correlation between I and Q components in the received signal. For a Gray mapping modulation, its normalized LLR (i.e., $\min_{a \in \mathcal{A}_k^1} (r_I/\rho_I - a_I)^2 - \min_{a \in \mathcal{A}_k^0} (r_I/\rho_I - a_I)^2$ for I channel) can be further reduced based on either piecewise linear approximation with an LLR coefficient table [15], [16] or pre-calculation of the closest points in each set of $\mathcal{A}_k^1$ and $\mathcal{A}_k^0$ [17]. However, the performance can be even worse than non-rotated QAM case, if we apply those algorithms directly to a rotated QAM case after simple de-rotation.

III. Proposed Soft-Demapping Algorithms for Rotated QAM

In this section, we propose 1D soft-demapping algorithms for the rotated QAM, to reduce its complexity as low as the complexity of the non-rotated QAM soft-demapper. The 1D soft-demapper of the non-rotated QAM is applicable to the rotated QAM with a pre-processing such as decorrelation between the channel coefficients of I and Q components. To get a good pre-processor, we reformulate the received rotated QAM signal as two PAM signals. Under the Gaussian approximation of the post decorrelated signals, this paper shows that the ML detection is simplified to MMSE decorrelation followed by 1D soft-demapping. The MMSE decorrelator can be the best pre-processor under the assumption, but there is residual interference in reality. To reduce the interference after MMSE decorrelation, we propose an MMSE decorrelator with IC as an another pre-processor. Fig. 2 illustrates the concept of our proposed 1D soft-demapping algorithms. The pre-processor can be either an MMSE decorrelator or an MMSE decorrelator with IC (MMSE-IC). The outputs of the pre-processor are defined by preprocessed received signals, $\hat{\mathbf{x}} = [\hat{x}_I, \hat{x}_Q]^T$, and soft-scalings, β_I and β_Q, where the soft-scalings are corresponding to signal-to-interference plus noise ratio (SINR) of the preprocessed signals. The normalized LLRs of Gray mapped PAM signals can be calculated by using the preprocessed received signals and

[5]Note that the channel coefficients are nearly independent, due to a cell interleaver after delayed Q component in the DVB-T2 system [3].

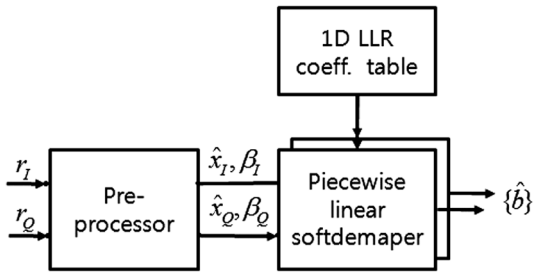

Fig. 2. Concept of the proposed soft-demapping algorithms for rotated QAM

predefined coefficient table, and they are scaled by the soft-scalings. Note that the soft-demapper of the non-rotated QAM has same procedure without the pre-processing. In non-rotated QAM case, the soft-scalings are corresponding to SNR. In two following subsections, more detail explanation of the proposed algorithms is given.

A. 1D Soft-demapping with an MMSE Decorrelation

As shown in (3), the system can be considered as a 2×2 multiple input multiple output (MIMO) system, where its corresponding channel matrix is given by

$$\mathbf{H} \triangleq \mathbf{PQ} = \begin{bmatrix} \rho_I & 0 \\ 0 & \rho_Q \end{bmatrix} \begin{bmatrix} \cos\theta & -\sin\theta \\ \sin\theta & \cos\theta \end{bmatrix}. \tag{8}$$

For a given channel matrix $\mathbf{H}$ with additive white Gaussian noise, the LLR given by (5) can be rewritten as

$$\Lambda(b_k) = \log\left(\frac{\sum_{\mathbf{x}:x_i \in \mathcal{A}^0_{k,i}} \exp\left(-\frac{2}{\sigma_n^2}\|\mathbf{r}-\mathbf{Hx}\|^2\right)}{\sum_{\mathbf{x}:x_i \in \mathcal{A}^1_{k,i}} \exp\left(-\frac{2}{\sigma_n^2}\|\mathbf{r}-\mathbf{Hx}\|^2\right)} \right), \tag{9}$$

where we separate all K bits into two groups (i.e., each group consists of $K/2$ bits for the PAM signal in real or imaginary axis). In the DVB-T2 specification, the real axis PAM signal consists of the odd kth bits and let $i = I$ for odd ks. In the same manner, let $i = Q$ for even ks. To match those subscripts to matrix and vector expressions, let the subscripts I and Q be 1 and 2, respectively. In addition, $\mathcal{A}^1_{k,i}$ and $\mathcal{A}^0_{k,i}$ denote a constellation set corresponding to the ith PAM signals whose $((k-i/2)+1)$th bit is 1 and 0, respectively. Let a zero-forcing equalized signal be $\hat{\mathbf{x}}_{ZF} \triangleq (\mathbf{H}^T\mathbf{H})^{-1}\mathbf{H}^T\mathbf{r}$. From the relation of $\|\mathbf{r}-\mathbf{Hx}\|^2 = (\hat{\mathbf{x}}_{ZF}-\mathbf{x})^T\mathbf{H}^T\mathbf{H}(\hat{\mathbf{x}}_{ZF}-\mathbf{x}) + \mathbf{r}^T(\mathbf{I}-\mathbf{H}(\mathbf{H}^T\mathbf{H})^{-1}\mathbf{H}^T)\mathbf{r}$ [18], the LLR can be express as

$$\Lambda(b_k) = \log\left(\frac{\sum_{\mathbf{x}:x_i \in \mathcal{A}^0_{k,i}} \exp\left(-\frac{2}{\sigma_n^2}\|\mathbf{H}(\hat{\mathbf{x}}_{ZF}-\mathbf{x})\|^2\right)}{\sum_{\mathbf{x}:x_i \in \mathcal{A}^1_{k,i}} \exp\left(-\frac{2}{\sigma_n^2}\|\mathbf{H}(\hat{\mathbf{x}}_{ZF}-\mathbf{x})\|^2\right)} \right) \tag{10}$$

$$= \log\left(\frac{\Pr(\hat{\mathbf{x}}_{ZF}|b_{k,i}=0)}{\Pr(\hat{\mathbf{x}}_{ZF}|b_{k,i}=1)} \right). \tag{11}$$

Due to the invariance of $\mathbf{r}^T(\mathbf{I}-\mathbf{H}(\mathbf{H}^T\mathbf{H})^{-1}\mathbf{H}^T)\mathbf{r}$ for a given $b_{k,i}$ (either 0 or 1), $\log(\Pr(\mathbf{r}|b_{k,i}=0)/\Pr(\mathbf{r}|b_{k,i}=1)) = \log(\Pr(\hat{\mathbf{x}}_{ZF}|b_{k,i}=0)/\Pr(\hat{\mathbf{x}}_{ZF}|b_{k,i}=1))$. From Bayes' rule and equiprobable bit distribution, (11) can be written as

$$\Lambda(b_k) = \log\left(\frac{\sum_{a_i \in \mathcal{A}^0_{k,i}} \Pr(\hat{\mathbf{x}}_{ZF}|x_i=a_i)}{\sum_{a_i \in \mathcal{A}^1_{k,i}} \Pr(\hat{\mathbf{x}}_{ZF}|x_i=a_i)} \right). \tag{12}$$

The max-log approximated LLR is given by

$$\Lambda(b_k) \approx \max_{a_i \in \mathcal{A}^0_{k,i}} \log\Pr[\hat{\mathbf{x}}_{ZF}|x_i=a_i] - \max_{a_i \in \mathcal{A}^1_{k,i}} \log\Pr[\hat{\mathbf{x}}_{ZF}|x_i=a_i]. \tag{13}$$

Gaussian approximation has been used for post detection interferences in either multi-user systems [19] or MIMO systems [20], due to its computational efficiency. In this paper, we also use the Gaussian approximation on the interference plus noise after zero-forcing equalization.

$$\Pr[\hat{\mathbf{x}}_{ZF}|x_i=a_i] \approx \frac{1}{2\pi\sqrt{\det\mathbf{C}_i}} \exp\left(-\frac{1}{2}(\hat{\mathbf{x}}_{ZF}-\boldsymbol{\mu}_i)^T\mathbf{C}_i^{-1}(\hat{\mathbf{x}}_{ZF}-\boldsymbol{\mu}_i)\right),$$
$$\text{with } \mu_i \triangleq a_i\mathbf{e}_i \text{ and } \mathbf{C}_i \triangleq \frac{1}{2}\left(\mathbf{I}-\mathbf{e}_i\mathbf{e}_i^T+\sigma_n^2(\mathbf{H}^T\mathbf{H})^{-1}\right), \tag{14}$$

where $\mathbf{e}_i$ is the ith 2D unit vector and 1/2 comes from real domain processing. The only difference of the soft-demapper for the rotated QAM compared with a soft-demapper for a 2×2 MIMO system comes from the different format of channel matrix and real domain processing. Based on the fact that the optimal LLR calculation for MIMO systems with the Gaussian assumption on post detection interference results in U-MMSE equalization followed by per-layer LLR calculation [20], the per-component soft-demapping (i.e., 1D soft-demapping) after the MMSE decorrelation can be written as,

$$\Lambda_{MMSE,i}(b_k) = \beta_i\left[\min_{a \in \mathcal{A}^1_{k,i}} \left| \frac{\hat{x}_{MMSE,i}}{\gamma_{ii}} - a_i \right|^2 - \min_{a \in \mathcal{A}^0_{k,i}} \left| \frac{\hat{x}_{MMSE,i}}{\gamma_{ii}} - a_i \right|^2 \right], \tag{15}$$

$$\text{where } \hat{x}_{MMSE,i} \triangleq \text{the } i\text{th component of } \hat{\mathbf{x}}_{MMSE},$$
$$\hat{\mathbf{x}}_{MMSE} \triangleq \left(\mathbf{H}^T\mathbf{H}+\sigma_n^2\mathbf{I}\right)^{-1}\mathbf{H}^T\mathbf{r},$$
$$\gamma_{ii} \triangleq \text{the } (i,i)\text{th diagonal term of } \boldsymbol{\Gamma},$$
$$\boldsymbol{\Gamma} \triangleq \left(\mathbf{H}^T\mathbf{H}+\sigma_n^2\mathbf{I}\right)^{-1}\mathbf{H}^T\mathbf{H},$$
$$\beta_i \triangleq \frac{\gamma_{ii}}{1-\gamma_{ii}}.$$

Due to the characteristic of the corresponding channel matrix, we do not require matrix inversion as follows.

$$\hat{\mathbf{x}}_{MMSE} = \mathbf{Q}^T\left(\mathbf{P}^2+\sigma_n^2\mathbf{I}\right)^{-1}\mathbf{P}^T\mathbf{r} = \mathbf{Q}^T\begin{bmatrix} \frac{\rho_I}{\rho_I^2+\sigma_n^2}r_I \\ \frac{\rho_Q}{\rho_Q^2+\sigma_n^2}r_Q \end{bmatrix}, \tag{16}$$

$$\boldsymbol{\Gamma} = \mathbf{Q}^T\left(\mathbf{P}^2+\sigma_n^2\mathbf{I}\right)^{-1}\mathbf{P}^2\mathbf{Q} = \mathbf{Q}^T\begin{bmatrix} \frac{\rho_I^2}{\rho_I^2+\sigma_n^2} & 0 \\ 0 & \frac{\rho_Q^2}{\rho_Q^2+\sigma_n^2} \end{bmatrix}\mathbf{Q}. \tag{17}$$

As shown in (16), the MMSE decorrelated signals are given by MMSE per component followed by de-rotation. Because the ith MMSE decorrelated signal $\hat{x}_{MMSE,i}$ is normalized

by its post detection signal power γ_{ii}, the soft-demapping measures "unbiased distance". The normalized LLR calculation $\left[\min_{a\in\mathcal{A}^1_{k,i}}\left|\frac{\hat{x}_{MMSE,i}}{\gamma_{ii}}-a_i\right|^2-\min_{a\in\mathcal{A}^0_{k,i}}\left|\frac{\hat{x}_{MMSE,i}}{\gamma_{ii}}-a_i\right|^2\right]$ can be calculated by piecewise linear soft-demapping with 1D LLR tables of slope and additive parts in a piecewise linear function as in [15]. Finally, the additional soft-scaling β_i is given by the post detection SINR.

1) The proposed 1D soft-demapping with an MMSE decorrelation is summarized as follows.
2) MMSE decorrelation: MMSE equalization per each I and Q component followed by de-rotation.
3) Normalization of two MMSE decorrelated signals by their post detection signal power γ_{ii}.
4) 1D soft-demapping for each component using 1D LLR coefficient tables.
   i. The U-MMSE decorrelated signal is scaled with the inverse of the normalization parameter per modulation order (i.e., $\frac{\hat{x}_{MMSE,i}}{\gamma_{ii}}$ is multiplied by $\sqrt{C}$, e.g., $C=170$ for 256-QAM).
   ii. Find a corresponding segment (e.g., the segment is one of $\{(-\infty,-14),[-14,-12),\cdots,[14,\infty)\}$ for 256-QAM). When the ith component falls in the lth segment, let the starting point of the corresponding segment be $\delta_i(l)$ except for the first segment. For 256-QAM, the first segment $\delta_i(1)\triangleq -16$.
   iii. Scale the difference $\sqrt{C}\frac{\hat{x}_{MMSE,i}}{\gamma_{ii}}-\delta_i(l)$ by the slope corresponding to the segment from the 1D LLR table of the slope in piecewise linear segments.
   iv. Add the scaled difference and the additive term corresponding to the segment from the 1D LLR table of additive terms in piecewise linear segments.
5) LLR scaling with SINR β_i per component and normalization with the square of the normalization parameter per modulation order.

B. 1D Soft-demapping With an MMSE Decorrelation With Interference Cancellation

Even though we can suppress interference by the MMSE decorrelation, still interference from the other channel exists as given in (17) due to rotation and de-rotation parts. To increase the post detection SINR of a weak component between I and Q components, we use IC. After selecting a stronger component between I and Q components [21], the component is detected first and then it is cancelled from the received signal to improve the post detection SINR of the weak component. Usually in the practical implementation of successive IC (SIC) [22], [23], the implementation of SIC is difficult to be parallelized due to the stronger component selection. Therefore, [22] considered SIC with power control to keep the same pipelined SIC structure and [23] proposed a parallel sorted QR decomposition instead of selecting maximum post SINR at the cost of BER performance. For the rotated QAM case, however, the selection is simplified because it is done by comparing SNR before the MMSE decorrelation as follows.

Remark: For $\forall\theta, 0\le\theta<\frac{\pi}{4}$, $\beta_I>\beta_Q$, if and only if $\rho_I>\rho_Q$, where β_I and β_Q denote post SINRs of an MMSE decorrelation for the rotated QAM. The proof of the statement is as mentioned below,

$$\begin{aligned}\beta_I-\beta_Q&=\frac{\rho_I^2\rho_Q^2+\sigma_n^2\left(\rho_I^2\cos^2\theta+\rho_Q^2\sin^2\theta\right)}{\sigma_n^4+\sigma_n^2\left(\rho_I^2\sin^2\theta+\rho_Q^2\cos^2\theta\right)}\\&\quad-\frac{\rho_I^2\rho_Q^2+\sigma_n^2\left(\rho_I^2\sin^2\theta+\rho_Q^2\cos^2\theta\right)}{\sigma_n^4+\sigma_n^2\left(\rho_I^2\cos^2\theta+\rho_Q^2\sin^2\theta\right)}\\&=g\left(\rho_I^2+\sigma_n^2\right)\left(\rho_Q^2+\sigma_n^2\right)\left(\cos^2\theta-\sin^2\theta\right)\left(\rho_I^2-\rho_Q^2\right),\end{aligned}\quad(18)$$

where $\cos^2\theta-\sin^2\theta$ is a positive value for $0\le\theta<\frac{\pi}{4}$ and g is also a positive value given by $\frac{1}{\sigma_n^2(\sigma_n^2+\rho_I^2\sin^2\theta+\rho_Q^2\cos^2\theta)(\sigma_n^2+\rho_I^2\cos^2\theta+\rho_Q^2\sin^2\theta)}$. Finally, $\beta_I>\beta_Q$, if and only if $\rho_I>\rho_Q$. Therefore, we can rearrange signal in advance for parallel processing especially implementing on a CGRA processor.[6]

Based on the SNRs ρ_I and ρ_Q, a strong component is selected first. In this paper, we call this as MMSE-IC2, whereas selecting the strong component based on the post SINR after an MMSE decorrelation is considered as MMSE-IC1. The LLRs of the bits corresponding to the selected component are calculated by (15) after an MMSE decorrelation. Let $\bar{a}_1$ and $\bar{a}_2$ be hard decision PAM signals based on U-MMSE decorrelated signals $\frac{\hat{x}_{MMSE,1}}{\gamma_{1,1}}$ and $\frac{\hat{x}_{MMSE,2}}{\gamma_{2,2}}$, respectively. The hard decision PAM signal corresponding to the selected component is cancelled from the received signal. Then the LLR for the other channel is calculated by

$$\begin{aligned}&\Lambda_{IC,i}(b_k)\\&=\beta_{IC,i}\left[\min_{a\in\mathcal{A}^1_{k,i}}\left|\frac{\hat{x}_{IC,i}}{\gamma_{IC,i}}-a_i\right|^2-\min_{a\in\mathcal{A}^0_{k,i}}\left|\frac{\hat{x}_{IC,i}}{\gamma_{IC,i}}-a_i\right|^2\right],\end{aligned}\quad(19)$$

$$\text{where } \hat{x}_{IC,i}\triangleq\frac{\mathbf{h}_i^T(\mathbf{r}-\mathbf{h}_j\bar{a}_j)}{\left(\mathbf{h}_i^T\mathbf{h}_i+\sigma_n^2\right)},\quad j\ne i\ \forall i,j=1\text{ or }2$$

$$\gamma_{IC,i}\triangleq\frac{\mathbf{h}_i^T\mathbf{h}_i}{\left(\mathbf{h}_i^T\mathbf{h}_i+\sigma_n^2\right)},$$

$$\beta_{IC,i}\triangleq\frac{\gamma_{IC,i}}{1-\gamma_{IC,i}}.$$

The procedure of the proposed 1D soft-demapping with MMSE-IC2 is as follows.

1) Select a stronger component between I and Q components based on their SNR.
2) MMSE decorrelation for the selected component and normalization with its post detection signal power γ_{jj}.
3) MMSE decorrelation with IC:
   i. Make a hard decision[7] $\bar{a}_i$ from the $\frac{\hat{x}_{MMSE,i}}{\gamma_{ii}}$.
   ii. Interference cancellation: $\mathbf{r}-\mathbf{h}_i\bar{a}_i$.
   iii. Calculate the normalized MMSE-IC output $\frac{\hat{x}_{IC,i}}{\gamma_{IC,i}}$.

[6]We will discuss the feature in detail in Section IV. Coarse-grained array (CGA) processor has been often referred as a coarse-grained reconfigurable array (CGRA) processor [12].

[7]A soft decision can be used. When a soft decision from the MMSE output is used (not from the decoder output as in an iterative detection and decoding structure), the performance improvement is too small to allow high complexity increase, compared with a hard decision.

4) 1D soft-demapping for each component (one component from Step 2 and the other component from Step 3) by using 1D LLR coefficient tables.
5) LLR scaling with SINRs $\beta_{MMSE,j}$ and $\beta_{IC,i}$, where $i \neq j$.

For the MMSE-IC1, the SINR calculation after MMSE should be done in Step 2 for the post detection SINR comparison (not SNR before pre-processing), and the order of step 1 and step 2 is interchanged. Note that the same 1D piecewise linear soft-demapping using 1D LLR tables is used for both proposed soft-demapping algorithms with MMSE and MMSE-IC. In addition, the 1D soft-demapping can be used for the non-rotated QAM without modification, where the pre-processing part is not required.

IV. Implementation on the CGRA Processor

The proposed algorithms are optimized on the CGRA processor. Section IV-A overviews the architecture of the CGRA processor and Section IV-B summarizes optimization points during implementation.

A. Architecture Overview of the Processor

The in-house CGRA processor used for the current implementation is based on an architecture for dynamically reconfigurable embedded systems (ADRES)[8] [12]. It is high speed reconfigurable array processor with rich set of instructions targeting wireless applications.

1) DSP Core: The core consists of a very long instruction word (VLIW) controller and the coarse-grained array (CGA) accelerator. Most data signal processing algorithms expressed in the form of for-loops are assigned to the CGA part while the VLIW controller is responsible for the general control of the CGA and simple sequential data processing. Fig. 3 shows the CGRA processor consists of 16 functional units (FUs) with an interconnection network connecting all the FUs, where the left-top 3 FUs are assigned for both VLIW controller and CGA accelerator. Each of the 16 FUs has 64-bit data width supporting either 4×16 bit or 2×32 bit single instruction multiple data (SIMD) processing. Note that 4×16 bit data can express 2 complex data samples of 32 bit each. Since the core has 16 FUs with 4-way SIMD, the best scheduling of the CGA process results in 64 operations per cycle.

2) Operating Modes in the Processor: Two exclusive operating modes are available according to VLIW controller and CGA accelerator. Since both modes share 3 FUs and register files, they cannot run concurrently. In VLIW mode, instructions are fetched from VLIW instruction cache as shown in Fig. 3, and decoded and executed as a typical 3-issued VLIW processor. In CGA mode, instructions are fetched from the configuration memory, decoded and executed concurrently in parts of 16 FUs. In this mode, the instruction-level parallelism (ILP) is maximized with the efficient software pipelining with proper scheduling of the interconnection among FUs. Note that both VLIW and CGA modes can utilize the SIMD architecture for maximum data-level parallelism (DLP).

[8]ADRES is a reconfigurable architecture, which tightly couples Very Long Instruction Word processor (VLIW) [24] and CGRA architecture [12] by providing two functional views on same physical resources. The architectures that involve CGRA technology are emerging as one of the potential candidates to meet the high performance, power efficiency and flexibility needed by current SDR systems [11], [25].

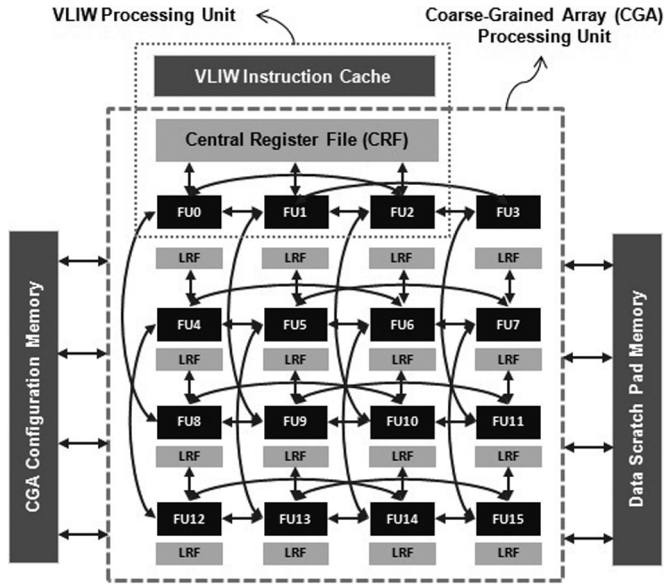

Fig. 3. Architecture [14]: The processor consists of 16 functional units (FUs) with 64-bit width each and has two operating modes (i.e., very long instruction word (VLIW) and coarse-grained array (CGA)).

B. Implementation of the Proposed Soft-Demapping Algorithms

There are two major performance measures of software implementation on the CGRA processor: output fidelity by means of signal to quantization noise ratio (SQNR) [26] and execution time by means of CGA cycles. The output fidelity is also measured with BER performance in addition to SQNR. The major factor that contributes towards SQNR is, number of coarse bits allocated for data and choosing the most accurate Q-format [27] for data under calculation. The other major factor that contributes towards CGA cycles is parallelizing the data processing using 64-bit SIMD instructions.

The Implementation of the soft-demapping algorithm involves various steps starting from algorithm design in MATLAB, to the optimized fixed point kernel for high throughput. The steps that were followed during the implementation of optimized fixed point kernel for soft-demapping on the CGRA processor are given.

1) Initially, the soft-demapping algorithm is implemented at MATLAB level as an algorithm proof.
2) After MATLAB implementation and corresponding BER curves are satisfied, the code is converted to floating point C code manually.
3) A fixed point model of the algorithm was created with the most accurate possible Q-format to achieve maximum possible SQNR. The SQNR is measured with the following formula.

$$\mathrm{SQNR} = 10\log_{10}\frac{\sum_n y^2[n]}{\sum_n \left(\hat{y}[n] - y[n]\right)^2}, \tag{20}$$

where y is LLR data from MATLAB output and $\hat{y}$ is fixed point(Q15.1) LLR output. The input parameters for the

TABLE I
CYCLE PERFORMANCE PER FEC BLOCK FOR 1D SOFT-DEMAPPING ALGORITHMS FOR A ROTATED 64-QAM ($\mathrm{EbN0} = 12.9$ dB IN MEMORYLESS RAYLEIGH CHANNEL WITHOUT ERASURE)

Algorithm	SQNR	CGA cycles	VLIW cycles	Total cycles	IPC	FU utilization
1D soft-demapping with MMSE	45.2dB	205607	108	205715	8.52	85%
1D soft-demapping with MMSE-IC1	44.1dB	335370	130	335500	7.29	90%
1D soft-demapping with MMSE-IC2	44.1dB	295204	170	295374	7.07	46%, 80%, 77% per loop

soft-demapping function are also in fixed point format. The output of the equalizer which forms as input to the soft-demapping function mainly I, Q components and channel state information (CSI) are packed together to form a 32 bit data before passing to the function and are unpacked in the soft-demapping function to individual variables.

4) Mapping and parallelization:
   - The soft-demapping algorithm was optimized using 64-bit SIMD intrinsics. This 4-way SIMD processing helps in calculating 4 LLR values simultaneously in case of 256-QAM and 3 LLR values simultaneously in case of 64-QAM. Also SIMD complex multiplication instructions were used for calculating the de-rotation of 2 symbols simultaneously, reducing 8 multiplications to 1 single parallel multiplication and 4 additions to 1 single addition, hence reducing the mathematical operations by factor of 12 altogether. These were the major part of the optimization.
   - Other optimizations include, using bitwise operations along with clipping intrinsics for finding the closest segment[9] instead of a function call, which further downloaded a segment table and used conditional operator to search the location of the segment, hence reducing expensive operations like memory access and conditional data flow. This was feasible since the limits of the segments were even numbers and were easily able to separate through least significant bit (LSB) masking. Similarly the distance calculation from the nearest constellation point, used in MMSE-IC, was calculated by LSB masking since the constellation points were easily able to separate by masking the LSBs.
   - Another important optimization was for LLR multiplexing (i.e., the reverse processing of bit to cell word de-multiplexing in the DVB-T2 specification [3]). LLR multiplexing was done within the main kernel instead of multiplexing externally hence avoiding an extra CGA loop. This is achieved by defining a pattern table in the code and using the table directly for the multiplexed indexes, while storing the LLR results to output buffers.
   - In case of division calculations, Liddicoat and Flynn approximation algorithm [28], [29] was used for the BER performance increase. Although Division intrinsics were readily available for the processor, the supported bit resolution (i.e., 24 bit division) was not enough, especially in the calculation of γ_{ii}. Hence the above division algorithm was used by having 32 bit resolution operations only for γ_{ii} calculation, because γ_{ii} is very sensitive for its accuracy (i.e., it is the input of the additional division for SINR calculation and SINR decides the scale of LLR).
5) The refinement of the code to achieve best SQNR and refinement of the code to achieve high speed performance were continued in loop for several iterations. The above steps are followed for MMSE and for MMSE-IC1 as given in Section III. Because the conditional selection of the stronger channel per each cell was inside the loop in case of MMSE-IC1, the scheduling of the loop with conditional execution was not efficient. Hence the selection criteria was moved outside the main loop forming a separate dedicated loop and calculation of the LLR values was further divided into two loops forming total three individual loops. This refined code was denoted as MMSE-IC2 as shown in Section III-B. This refinement was done through MATLAB code re-design, followed by floating point design refinement, fixed point code refinement and further updating the parallelized code. Because of this, there was around 12% gain in terms of total performance without affecting SQNR.

Table I shows the performance details of MMSE, MMSE-IC1 and MMSE-IC2 fixed point soft-demappers implemented on the CGRA processor in 64-QAM case. CGA cycles refer to the number of processor clock cycles needed to execute the soft-demapping algorithm on the processor in CGA mode. As shown in Table I, 99% of the code is executed in CGA mode which mainly consists of data massive part. VLIW cycles refer to the processor clock cycles needed to execute the soft-demapping function control flow. Since VLIW cycles account only for control code, the contribution in terms of speed is almost ignorable when compared to CGA mode which executes data massive part. Instructions per cycle (IPC) refers to the average number of instructions executed per cycle in CGA mode. Higher IPC indicates high level of parallelism and good scheduling. FU utilization refers to the percentage of the processor utilization against the power spent to execute one CGA loop.

Since in case of MMSE-IC2 the main demapping loop has been divided into three separate loops, there are three separate data in terms of FU utilization, however IPC has been averaged and all the cycle numbers are added across all three loops. For MMSE-IC2, although there is 30% degradation in VLIW cycles due to extra control code of the extra loops, it is completely ignorable when compared to total performance gain with respect to MMSE-IC1 and the total gain is 12%.

[9]Please refer the procedure of the 1D soft-demapping using LLR tables in Section III-A.

TABLE II
SNR GAP COMPARISON OF LOW COMPLEXITY SOFT-DEMAPPING ALGORITHMS COMPARED TO THE FULL SEARCH ALGORITHM IN A 0 dB SINGLE ECHO CHANNEL AT 26.6 μs: SNR GAP AT 10^{-3} BER

	64-QAM				256-QAM			
	3/5	2/3	4/5	5/6	3/5	2/3	4/5	5/6
2D rotated-L-shape sub-region (subset 1) [7]	0.01	0.01	0.03	0.06	0.01	0.01	0.01	0.01
2D square-shape sub-region [8]	0.08	0.12	0.44	0.68	0.01	0.01	0.08	0.16
1D soft-demapping with MMSE-IC	0.01	0.04	0.23	0.43	0.01	0.01	0.02	0.04
1D soft-demapping with MMSE	0.01	0.04	0.44	0.66	0.01	0.01	0.08	0.11

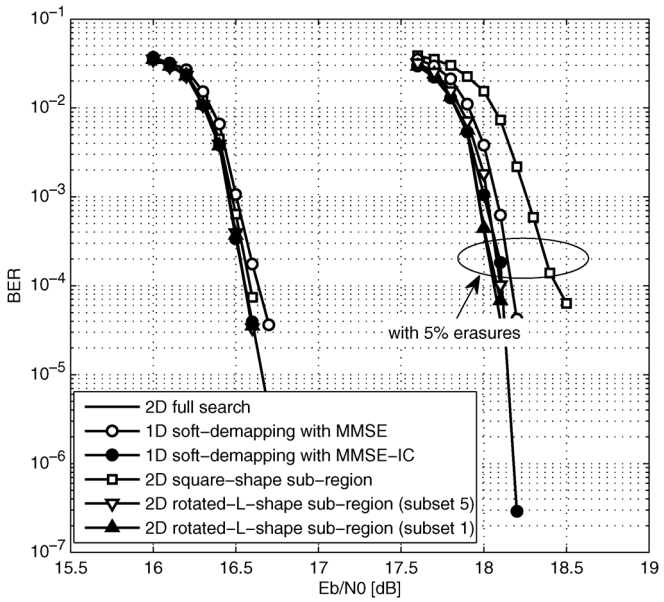

Fig. 4. BER performance comparison of soft-demapping algorithms for a rotated 256-QAM with 4/5 code rate in memoryless Rayleigh channels with/without erasure events.

V. PERFORMANCE EVALUATION

In this section, we evaluate the performance of the proposed algorithms compared with previously known soft-demapping algorithms for the rotated QAM in terms of BER and complexity, where the required number of operations and required cycles per second (cps) are compared.

A. Bit Error Rate Performance

To evaluate the performance of the proposed algorithms, we perform a set of simulations in a memoryless Rayleigh channel with/without erasures [4], [8] and a 0 dB single echo channel at 26.6 μs [5]. A low density parity check (LDPC) code with 3/5, 2/3, 4/5, and 5/6 code rates is used, where the forward error correction (FEC) block size is 64800 bits. Modulation specific rotation angles defined in the DVB-T2 specification [3] are considered. For the 1D soft-demapping, we use look-up tables[10] containing slope and additive information of the normalized LLR. For a 2^m-QAM signal, the two tables with size $\frac{m}{2} \times 2^{m/2}$ can express the normalized LLR exactly, which is distinct from the approximated version in [15].

[10]For example, the two tables for a 256-QAM signal are given as Tables V and VI in Appendix A.

In Fig. 4, the BER performance of the proposed algorithms in a 256-QAM case is compared with the full search algorithm and two 2D sub-region based algorithms (i.e., the rotated-L-shape [7] and square-shape sub-regions [8]). Without erasure events, the BER performance of the 1D soft-demapping with MMSE-IC is almost same with the full search algorithm, similar to 2D sub-region based algorithms. In addition, the performance gap between the 1D soft-demapping with MMSE and the full search algorithm is less than 0.1 dB at 10^{-3} BER. In 5% erasure channels, we can see clearly the BER performance difference according to different soft-demapping algorithms. Among sub-region based algorithms, the rotated-L-shape sub-region (subset 1) shows the best performance. The performance of the rotated-L-shape sub-region (subset 5)[11] is worse than the performance of the sub-region (subset 1), but it is better than the square-shape sub-region based algorithm. The proposed 1D soft-demapping with MMSE-IC is better than the square-shape sub-region based algorithm in Rayleigh channel with 5% erasure events. The performance gap of the 1D soft-demapping with MMSE or MMSE-IC is less than 0.15 dB compared with the full search algorithm at 10^{-3} BER even in Rayleigh channel with 5% erasure events.

Table II compares the SNR gap between low complexity algorithms and the full search algorithm according to different code rate and modulation order in a 0 dB single echo channel. For all low complexity algorithms, the SNR gap increases with code rate and decreases with modulation order. Lower modulations have larger rotation angle (i.e., more correlation between I and Q components) than higher modulations. The increased correlation makes more diversity gain in the full search algorithm, whereas it causes more interference in 1D soft-demapping algorithms and diversity gain loss in sub-region based algorithms. In this comparison, only subset 1 is taken into account for the rotated-L-shape sub-region. It shows best performance and the SNR gap is less than 0.1 dB for all the eight cases in Table II. Similar to the results in Rayleigh channels with erasure events given in Fig. 4, the square-shape sub-region based algorithm shows worse performance in most 64-QAM cases and a 256-QAM case with 5/6 code rate and similar performance in the other cases, compared with the 1D soft-demapping with MMSE in a 0 dB single echo channel [5]. Overall, the SNR gaps of the square-shape sub-region based algorithm and 1D soft-demapping algorithm with MMSE are larger than 0.5 dB only in case of 64-QAM with 5/6 code rate.

[11]The rotated-L-shape sub-region (subset 5) is only available for 256-QAM [7]. The complexity is as low as 50% of the full search algorithm, whereas the complexity of the sub-region (subset 1) is 75% of the full search algorithm.

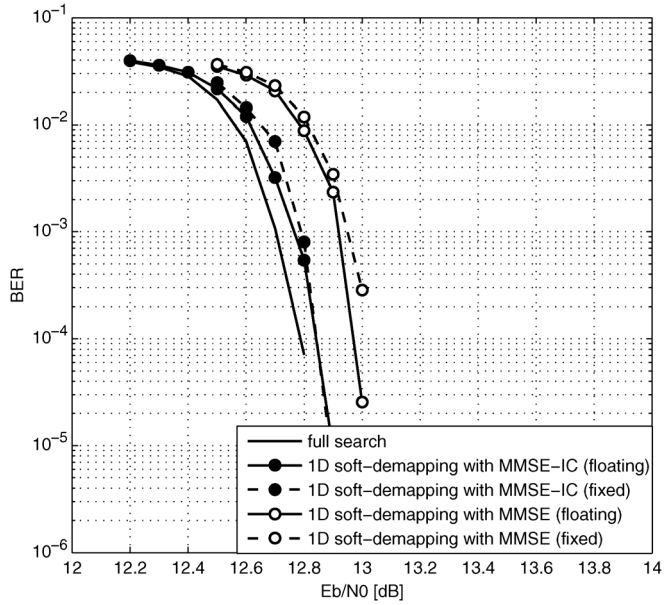

Fig. 5. BER performance comparison (fixed point and floating point simulation) of soft demapping algorithms for the rotated 64-QAM with 4/5 code rate in memoryless Rayleigh channels without erasure events.

In Fig. 5, fixed and floating point BER performances of the proposed algorithms compared with the full search algorithm for the rotated 64-QAM case. As explained, the performance gap of the proposed algorithms compared to the full search algorithm increases because of the larger rotation angle in 64-QAM than in 256-QAM. Compared with the full search algorithm, the SNR gaps of 1D soft-demapping with MMSE-IC and MMSE are less than 0.1 dB and 0.3 dB at 10^{-3} BER, respectively. The performance gap between floating point and fixed point is less than 0.05 dB.

B. Complexity Comparison

In terms of complexity, the proposed algorithm has much less complexity than not only the full search algorithm but also the sub-region based algorithms [7]–[9] especially for higher modulation orders. The detail comparison is given in Table III. The required number of multiplications and divisions per bit for a 2^m-QAM constellation is summarized, where the number of multiplications are counted for Euclidean distance calculation from the selected constellation points. For one 2D Euclidean distance calculation, 4 real multiplications are required. In the full search case, all Euclidean distances between a received signal and each of constellation points are calculated. The sub-region based algorithms calculate a part of the constellation points. There is only difference in the number of Euclidean distance calculation when the complexity of sub-region based algorithms is compared with one of the full search algorithm. For example, the square-shape sub-region based algorithm requires about 40% and 31% of full search complexity in 64-QAM and 256-QAM cases, respectively, and the rotated-L-shape sub-region based algorithm (subset 1) needs 75% of the full search algorithm complexity regardless of modulation order. Since the Euclidean distance calculation for the first bit can be reused in the LLR calculation for the other bits, complexity per bit can be normalized by the number of bits. Even though Euclidean distance calculation can be done once per symbol, the complexity per bit of the full search and sub-region based algorithms increase proportional to the constellation size. The complexity per bit of the proposed algorithms, however, decreases because the decorrelation and IC are executed in a symbol level. To clarify the computational cost in detail, we show the number of multiplications and divisions in each step of the proposed algorithms in Appendix A. Due to the simplicity of the 1D soft-demapping, the complexity of proposed algorithms is less than 5.5% for a 256-QAM and less than 20% for a 64-QAM compared to the complexity of the full search algorithm, where we considered the complexity of division as three times higher than the complexity of multiplication. Based on the both BER performance and complexity comparison, the proposed algorithm has more benefit for higher modulation order (i.e., the MMSE-IC based algorithm shows almost same BER performance with the full search algorithm only with its 5.5% complexity, especially for a 256-QAM).

TABLE III
COMPLEXITY COMPARISON: THE REQUIRED NUMBER OF MULTIPLICATIONS OR DIVISIONS FOR THE ONE BIT LLR CALCULATION OF A 2^m-QAM SIGNAL

Algorithm Description	MUL	DIV
2D full search	$\frac{4}{m} \cdot 2^m + 1$	
2D rotated-L-shape (subset 1) [7]	$\frac{3}{m} \cdot 2^m + 1$	
2D square-shape sub-region [8]	$\frac{4}{m} \cdot \left(2^{m/2-1} + 1\right)^2 + 1$	
1D soft-demapping with MMSE	$2 + \frac{18}{m}$	$\frac{6}{m}$
1D soft-demapping with MMSE-IC	$2 + \frac{23}{m}$	$\frac{5}{m}$

More accurate complexity comparison based on the implementation results on the processor is given in Fig. 6. The actual complexity of the proposed algorithms increases to 8% from 5.5% (i.e., given in Table III) of the full search algorithm complexity when 1D soft-demapping with MMSE-IC2 is used in 256-QAM case. One of main reasons is high resolution division. The required cycles according to modulation order slightly increases due to higher transmission data-rate, even though proposed algorithms have less complexity per bit for larger modulation order as shown in Table III. However the complexity of the proposed algorithms increases linearly (not exponentially as existing soft-demapping algorithms) and complexity itself is still less than 8% of the full search algorithm in a 256-QAM case. By dealing with the conditional execution outside of main loop based on (18), MMSE-IC2 can reduce about 30 Mcps (i.e., 12% complexity reduction in a 64-QAM case) compared to MMSE-IC1 without any BER performance loss. The both proposed algorithms can be implemented within 200 Mcps even in 256-QAM case. When we consider both cycle and BER performance, the proposed algorithms are more appropriate for higher modulation. For QPSK, the full search algorithm is the best choice in terms of complexity and BER performance.

Finally, Fig. 7 shows the implementation results of core kernels in the DTG106 mode, where the proposed 1D soft-demapping with the MMSE decorrelation is used. Even with the low

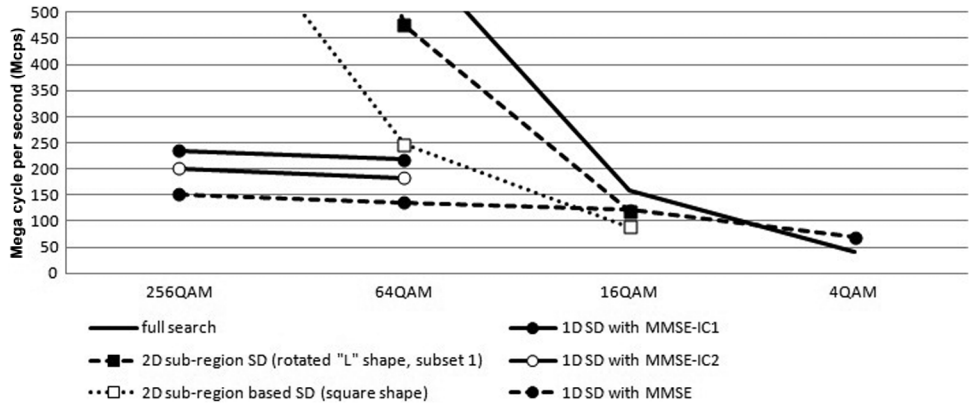

Fig. 6. The required cycles per second vs. modulation order according to soft-demapping algorithms. The proposed algorithms are implemented on the CGRA processor. As a reference, the complexity of the sub-region based soft-demapping and full search algorithm in the other modulation cases is estimated from the implementation result of the full search algorithm in QPSK case on the processor. Please note that the cycles for the 2D algorithms is underestimated. In the estimation, only the number of Euclidean distance calculations is considered (i.e., minimum selection in different sets for each bit and sub-region selection are not taken into account for the 2D algorithms. In addition, the output LLR arrangement by de-multiplexing given in the DVB-T2 system is only reflected for the cycles of the proposed algorithms.).

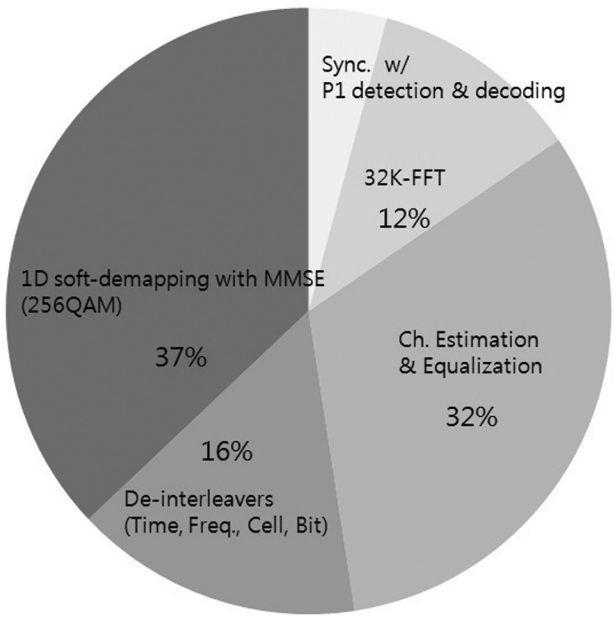

Fig. 7. Core kernel complexity ratio of the DTG106 mode in a DVB-T2 system based on the implementation results on the processor, when the proposed 1D soft-dempping with MMSE decorrelation is considered for a rotated 256-QAM signal. In total, 409 Mcps is required for the mapping of core kernels.

complexity softdemapper, the soft-demapping in a 256-QAM case shows 37% complexity of the total kernels of baseband modem excluding channel decoders. Compared with the result in [14], only the soft-demapping part is changed. The complexity of the proposed soft-demapper for a rotated 256-QAM is about double complexity of the soft-demapper for a non-rotated 256-QAM. If we consider the full search based soft-demapper, the total cycles will be over than 1.53 Giga cycles per second (Gcps) based on the cycle estimation in Fig. 6. Due to the proposed algorithm, we reduce total cycles to 409 Mcps from 1.53 Gcps (i.e., 73% reduction in total cycles). Even if about 50% margin is considered, only one 600 MHz processor is required for the DTG106 mode implementation.

TABLE IV
THE REQUIRED NUMBER OF MULTIPLICATIONS OR DIVISIONS FOR THE ONE BIT LLR CALCULATION OF A 2^m-QAM SIGNAL: 1D SOFT-DEMAPPING WITH AN MMSE DECORRELATION

Steps	description	MUL	DIV
MMSE decorrelation	MMSE filter coefficient	$2/m$	$2/m$
	MMSE equalization	$2/m$	
	derotation	$4/m$	
Normalization	γ_{ii}	$6/m$	
	normalization with γ_{ii}		$2/m$
Normalized LLR	scaling with $\sqrt{C}$	$2/m$	
	slope from a 1D LLR table	1	
LLR scaling with SINR	β_i		$2/m$
	β_i/C	$2/m$	
	scaling with β_i/C	1	

VI. CONCLUSION

In this paper, we proposed 1D soft-demapping algorithms using MMSE decorrelation and MMSE decorrelation with IC. Based on the reformulation of a received rotated QAM signal as two PAM signals, we derived that the ML detector is simplified to 2×2 MMSE decorrelation followed by 1D soft-demapping under Gaussian approximation on interference. To reduce residual interference from the other channel, IC is taken into account. By deriving the algorithms only for the rotated QAM, the proposed algorithms do not require matrix inversion, and the ordering of IC can be processed outside of main loop for parallel processing especially for the implementation on the CGRA processor. In addition, the 1D soft-demapping is simplified by table based LLR calculation. Therefore the proposed 1D soft-demapping with pre-processing (i.e., MMSE or MMSE-IC) shows less than 0.15 dB difference at 10^{-3} BER compared with the full search algorithm while the complexity is less than 8% of the full search algorithm in a 256-QAM case with any code rates. Due to the significantly reduced complexity of the proposed

TABLE V
TABLE OF LLR SLOPE INFORMATION PER SEGMENT IN 256-QAM CASE

segment point($\delta_i(l)$)	-16	-14	-12	-10	-8	-6	-4	-2	0	2	4	6	8	10	12	14
0th bit	32	28	24	20	16	12	8	4	4	8	12	16	20	24	28	32
1st bit	-16	-12	-8	-4	-4	-8	-12	-16	16	12	8	4	4	8	12	16
2nd bit	-8	-4	-4	-8	8	4	4	8	-8	-4	-4	-8	8	4	4	8
3rd bit	-4	-4	4	4	-4	-4	4	4	-4	-4	4	4	-4	-4	4	4

TABLE VI
TABLE OF LLR ADDITIVE TERM PER SEGMENT IN 256-QAM CASE

segment point($\delta_i(l)$)	-16	-14	-12	-10	-8	-6	-4	-2	0	2	4	6	8	10	12	14
0th bit	-288	-224	-168	-120	-80	-48	-24	-8	0	8	24	48	80	120	168	224
1st bit	80	48	24	8	0	-8	-24	-48	-80	-48	-24	-8	0	8	24	48
2nd bit	24	8	0	-8	-24	-8	0	8	24	8	0	-8	-24	-8	0	8
3rd bit	8	0	-8	0	8	0	-8	0	8	0	-8	0	8	0	-8	0

algorithms, the DTG106 mode can be implemented with one 600 MHz CGRA processor.

APPENDIX A

A. Complexity of Proposed Soft-Demapping Algorithms Using 1D LLR Tables

Table IV shows the complexity in each step of the proposed 1D soft-demapping with an MMSE decorrelation, where we assume that channel gain ρ_I, ρ_Q and noise variance σ_n^2 and its inverse $1/\sigma_n^2$ are given. According to modulation orders, the normalization parameters $1/C$ and $\sqrt{C}$, and rotation parameters $\cos\theta$, $\sin\theta$, $\cos^2\theta$, $\sin^2\theta$ and $\cos\theta\sin\theta$ are also given. Only the number of multiplications and divisions is summarized in this paper.

The number of multiplications and divisions are normalized by m, because we need an MMSE equalization and calculation of signal power γ_{ii} and SINR β_i per symbol. The normalized LLR calculation from 1D LLR tables and scaling of the normalized LLR with SINR require multiplications per bit. As in [15] and [16], the normalized LLR is composed of piecewise linear functions. In this paper, we store slope and additive information per each segment of the piecewise linear functions. For example, 1D LLR tables for 256-QAM in DVB-T2 are given by Tables V and VI. After finding the closest segment, we can calculated the normalized LLR with these two tables.

With same given information as in Table IV, the required number of multiplications or divisions in each step of the proposed 1D soft-demapping with MMSE-IC2 is summarized in Table VII. By combining MMSE-IC decorrelation and normalization, we can reduce the number of multiplications and divisions. If I channel gain is larger, let its hard decision signal from the normalized MMSE signal be $\bar{a}_I$. The normalized MMSE-IC signal of the Q channel is given by

$$\frac{\hat{x}_{MMSE-IC,Q}}{\gamma_Q} = \frac{-\rho_I \sin\theta r_I + \rho_Q \cos\theta r_Q + (\rho_I^2 - \rho_Q^2)\sin\theta\cos\theta\bar{a}_I}{\rho_I^2\sin^2\theta + \rho_Q^2\cos^2\theta}, \quad (21)$$

TABLE VII
THE REQUIRED NUMBER OF MULTIPLICATIONS OR DIVISIONS FOR THE ONE BIT LLR CALCULATION OF A 2^m-QAM SIGNAL: 1D SOFT-DEMAPPING WITH AN MMSE-IC2

Steps	description	MUL	DIV
MMSE (stronger ch.)	MMSE filter coefficient	$2/m$	$2/m$
	MMSE equalization	$2/m$	
	derotation	$2/m$	
MMSE normalization	γ_{jj}	$4/m$	
	normalization with γ_{jj}		$1/m$
MMSE-IC (weaker ch.)	normalized MMSE-IC	$8/m$	$1/m$
Normalized LLR	scaling with $\sqrt{C}$	$2/m$	
	slope from 1D LLR table	1	
LLR scaling with SINR	β_i	$1/m$	$1/m$
	β_i/C	$2/m$	
	scaling with β_i/C	1	

where ρ_I^2 and ρ_Q^2 are already calculated in the MMSE decorrelation. Without the calculation of γ_Q, the SINR is given by

$$\beta_Q = \frac{\rho_I^2\sin^2\theta + \rho_Q^2\cos^2\theta}{\sigma_n^2}. \quad (22)$$

The normalized LLR calculation and LLR scaling with SINR are same with Table IV.

REFERENCES

[1] X. Giraud, E. Boutillon, and J. Belfiore, "Algebraic tools to build modulation schemes for fading channels," *IEEE Trans. Inf. Theory*, vol. 43, no. 3, pp. 938–952, May 1997.

[2] J. Boutros and E. Viterbo, "Signal space diversity: A power- and bandwidth-efficient diversity technique for the Rayleigh fading channel," *IEEE Trans. Inf. Theory*, vol. 44, no. 4, pp. 1453–1467, Jul. 1998.

[3] *DVB-T2, Digital Video Broadcasting (DVB): Frame Structure Channel Coding and Modulation for a Second Generation Digital Terrestrial Television Broadcasting System*, ETSI EN 302 755, v1.1.1, Sep. 2009.

[4] A. Nour, Charbel, and Douillard, "Rotated QAM constellations to improve BICM performance for DVB-T2," in *Proc. Int. Symp. Spread Spectrum Tech. Appl.*, Aug. 2008, pp. 354–359.

[5] *BlueBook, Digital Video Broadcasting (DVB); Implementation Guidelines for a Second Generation Digital Terrestrial Television Broadcasting System*, ETSI A133, Jun. 2010.
[6] P. Robertson, E. Villebrun, and P. Hoeher, "A comparison of optimal and sub-optimal MAP decoding algorithms operating in the log domain," in *Proc. IEEE Int. Conf. Commun.*, Jun. 1995, vol. 2, pp. 1009–1013.
[7] D. Perez-Calderon, V. Baena-Lecuyer, A. Oria, P. Lopez, and J. Doblado, "Rotated constellation demapper for DVB-T2," *IEE Electron. Lett.*, vol. 47, no. 1, pp. 31–32, Jun. 2011.
[8] M. Li, C. Nour, C. Jego, and C. Douillard, "Design of rotated QAM mapper/demapper for the DVB-T2 standard," in *Proc. IEEE Workshop Signal Process. Syst.*, Oct. 2009, pp. 018–023.
[9] S. Tomasin and M. Butussi, "Low complexity demapping of rotated and cyclic Q delayed constellations for DVB-T2," *IEEE Wireless Commun. Lett.*, vol. 1, no. 2, pp. 81–84, Apr. 2012.
[10] M. Saleh, M. Sadek, and S. El Ramly, "Novel hybrid soft-hard demodulation schemes for RQD constellation," in *Proc. Int. Conf. Telecommun. Signal Process.*, Jul. 2012, pp. 684–688.
[11] B. MEI, "A coarse-grained reconfigurable architecture template and its compilation techniques," Ph.D. dissertation, Katholieke Universiteit Leuven, Leuven, Belgium, 2005 [Online]. Available: https://lirias.kuleuven.be/handle/123456789/66294
[12] S. Vassiliadis and D. Soudris, *Fine- and Coarse-Grain Reconfigurable Computing*. New York, NY, USA: Springer, 2007.
[13] S. Gauntlett, *Digital Terrestrial Television, Requirements for Interoperability (The D-Book),* Issue 6.1. London, U.K.: Digital TV Group, Mar. 2009.
[14] N. Basutkar, H. Yang, P. Xue, K. Bae, and Y.-H. Park, "Software-defined DVB-T2 receiver using coarse-grained reconfigurable array processors," in *Proc. IEEE Int. Conf. Consum. Electron.*, 2013, pp. 580–581.
[15] F. Tosato and P. Bisaglia, "Simplified soft-output demapper for binary interleaved COFDM with application to HIPERLAN/2," in *Proc. IEEE Int. Conf. Commun.*, Oct. 2002, vol. 2, pp. 664–668.
[16] E. Akay and E. Ayanoglu, "Low complexity decoding of BICM STBC," in *Proc. IEEE Veh. Technol. Conf.*, May 2005, vol. 2, pp. 715–718.
[17] D. Lin, Y. Xiao, and S. Li, "Low complexity soft decision technique for gray mapping modulation," *Wireless Pers. Commun.*, vol. 52, pp. 383–392, Jan. 2010.
[18] B. Hochwald and S. ten Brink, "Achieving near-capacity on a multiple-antenna channel," *IEEE Trans. Commun.*, vol. 51, no. 3, pp. 389–399, Mar. 2003.
[19] J. Luo, K. Pattipati, P. Willett, and F. Hasegawa, "A PDA approach to CDMA multiuser detection," in *Proc. IEEE Global Telecommun. Conf.*, Dec. 2001, vol. 2, pp. 763–766.
[20] D. Seethaler, G. Matz, and F. Hlawatsch, "An efficient MMSE-based demodulator for MIMO bit-interleaved coded modulation," in *Proc. IEEE Glob. Telecommun. Conf.*, Nov. 2004, vol. 4, pp. 2455–2459.
[21] P. Wolniansky, G. Foschini, G. Golden, and R. Valenzuela, "V-BLAST: An architecture for realizing very high data rates over the rich-scattering wireless channel," in *Proc. IEEE Int. Symp. Signals, Syst., Electron.*, Sep. 1998, pp. 295–300.
[22] K. Pedersen, T. Kolding, I. Seskar, and J. Holtzman, "Practical implementation of successive interference cancellation in DS/CDMA systems," in *Proc. IEEE Int. Conf. Univers. Pers. Commun.*, Sep. 1996, vol. 1, pp. 321–325.
[23] D. Wübben and K.-D. Kammeyer, "Low complexity successive interference cancellation for per-antenna-coded MIMO-OFDM schemes by applying parallel-SQRD," in *Proc. IEEE Veh. Technol. Conf.*, May 2006, vol. 5, pp. 2183–2187.
[24] J. A. Fisher, "Very long instruction word architectures and the ELI-512," in *Proc. 10th Annu. Int. Symp. Comput. Architect.*, 1983, pp. 140–150.
[25] O. Anjum, T. Ahonen, F. Garzia, J. Nurmi, C. Brunelli, and H. Berg, "State of the art baseband DSP platforms for software defined radio: A survey," *EURASIP J. Wireless Commun. Netw.*, June 2011.
[26] T. Aamodt, "Floating-point to fixed-point compilation and embedded architectural support," M.S. thesis, Univ. of Toronto, Toronto, ON, Canada, 2001 [Online]. Available: http://citeseerx.ist.psu.edu/viewdoc/summary?doi=10.1.1.26.5869
[27] E. L. Oberstar, "Fixed point representation & fractional math," Oberstar Consulting, Madison, WI, USA, Tech. Rep., 2007 [Online]. Available: http://www.superkits.net/whitepapers.htm
[28] T. J. Kwon and J. Draper, "Floating-point division and square root implementation using a Taylor-series expansion algorithm with reduced look-up tables," in *Proc. 51st Midwest Symp. Circuits Syst.*, Aug. 2008, pp. 954–957.
[29] A. Liddicoat and M. Flynn, "High-performance floating point divide," in *Proc. Euromicro Symp. Digit. Syst., Des.*, Sep. 2001, pp. 354–361.

Kyeongyeon Kim (S'06–M'10) received the B.S., M.S. and Ph.D. degrees in electrical engineering from Yonsei University, Seoul, Korea, in 2001, 2003 and 2007, respectively. After graduation, she was a postdoctoral fellow in Purdue University from 2007 to 2008 and in University of Illinois at Urbana-Champaign from 2008 to 2010. Since 2010, she joined Samsung Advanced Institute of Technology (SAIT), Samsung Electronics, Korea and has participated in low-power receiver algorithm design and software implementation of wireless communication and broadcasting systems. Her research interests include signal processing for wireless/underwater communication and broadcasting systems, array signal processing, and analysis and design of communication systems.

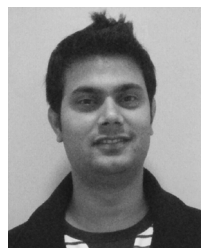

Navneet Basutkar received Bachelor of Engineering Degree in Electronics and Communication from Visvesvaraya Technological University, India, in 2005. He joined Samsung Electronics in 2010 and currently working as Research Staff for Software Defined Radio applications mainly in Wireless Communations domain. Before joining Samsung Electronics, he worked for Sasken Communication Technologies ltd., Bangalore, India, from 2006 to 2010. His research interests include real time processing of signal processing algorithms and instruction design for Digital Signal Processors.

Kitaek Bae (S'04–M'10) received his B.S. degree in Control and Instrumentation Engineering and a M.S. degree in Electronics Engineering from Chung-Ang University, Seoul, Korea, in 1995 and 1997, respectively, and the Ph.D. degree in Electrical and Computer Engineering from The University of Texas at Austin, in 2010. From 1997 to 2003, he was a Senior Engineer at LG Innotek, Inc., Seoul, Korea, where he worked on signal processing for sonar applications. He is now with Samsung Advanced Institute of Technology (SAIT), Gyunggi-do, South Korea. His research interests include PAR reduction in multicarrier systems; nonlinear signal processing, such as linearization of power amplifier, and DSP embedded software design for wireless communications including channel estimation, equalization, and soft-demapping.

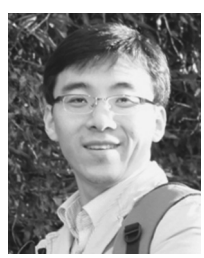

Peng Xue (S'07–M'10) received the B.E. degree in electronic information engineering from Shandong University, Jinan, China, in 2004 and the M.E. and Ph.D. degrees in information and communication engineering from Inha University, Incheon, Korea, in 2006 and 2010, respectively. In September 2010, he joined Samsung Advanced Institute of Technology, Korea, contributing to the transceiver design and algorithm development of next-generation wireless systems based on multiple-input multiple-output orthogonal frequency division multiplexing technology. His research interests also include radio resource management and crosslayer design of the wireless networks.

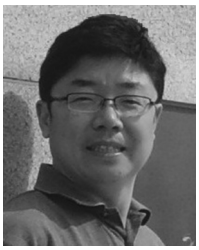

Ho Yang (S'96–M'02) received the B.S. and M.S. degrees from Yonsei University, Seoul, Korea, and the Ph.D. degree from the Georgia Institute of Technology, Atlanta, USA, all in electrical engineering in 1987, 1989 and 1998, respectively. From 1988 to 1989, he was a Research Engineer at the Department of Biomedical Engineering, Yonsei University College of Medicine, Seoul, Korea. From 1989 to 1991, he was a Research Engineer at the Electronics and Telecommunications Research Institute, Taejon, Korea. From 1999 to 2001, he was a Senior DSP Engineer with Nixxo technologies, San Jose, USA, where he was involved with the design of GSM modem. He joined Samsung Electronics, Yongin, Korea, in 2001. He is currently a principal research engineer leading the design activities of software-based baseband radio processor and platform. His research interests are signal processing algorithm, embedded software design, and DSP processor design for wireless modems including digital broadcasting receivers.